Importance of the Johnson-Cook Material Model Parameters in Simulation Studies of the Cutting Process

Marian Bartoszuk, Piotr Löschner

Department of Manufacturing Engineering and Automation, Opole University of Technology, Opole, POLAND
e-mails: m.bartoszuk@po.edu.pl; p.loschner@po.edu.pl

SUMMARY

Computer simulations of various manufacturing processes have become increasingly common in recent years. In machining, their primary goal is to rationalize the planning of experimental studies and to observe phenomena occurring in the cutting zone that cannot be observed otherwise. Another significant aspect is the ability to numerically verify many different process variants before conducting an experiment. Simulations are run based on an appropriate material model describing the tribomechanical behaviour of the material. Typically, this is the Johnson-Cook model, represented by five numerical parameters. However, to properly select the J-C model for calculations, one must understand how individual parameters affect the final simulation outcome. This study shows that it is possible to select many different sets of J-C model parameters that meet the equation conditions but yield different simulation results. Therefore, this paper shows the influence of individual numerical parameters of the J-C model on the simulation results, such as cutting forces, temperature distribution, chip morphology, etc. The tests and analyses presented in this paper were performed for AISI 321 austenitic steel.

KEY WORDS: *machining; numerical simulations; material model; J-C model parameters.*

1.   INTRODUCTION

Generally, numerical modelling is increasingly used in machining. to understand better phenomena that are difficult or costly to study experimentally [1]. Experimental studies, of course, provide much valuable data about the process. However, they primarily serve to verify phenomena observed in simulations and confirm the assumptions made in calculations and analyses. Literature analysis indicates that many different simulation methods are used in computer simulations of the cutting process [2]. The most popular methods include the finite difference method (FDM), the finite element method (FEM), the boundary element method (BEM), and smoothed particle hydrodynamics (SPH). The finite difference method is based on calculating the intensity of heat sources and is usually used to determine temperature fields in

examined sub-areas of the cutting zone. According to Grzesik [3], the material's constitutive model is unnecessary for these calculations. In other computational methods, the constitutive model is the basis of calculations, and its accuracy has a direct and significant impact on the obtained results and their precision. Literature analysis clearly shows that the Johnson-Cook material model is most commonly used in simulations of the cutting process [4]. For instance, Wu et al. [5] used the finite element method to simulate the chip formation and breaking process when turning AISI 1045 steel. FEM can also be used to solve more complex issues. A good example is the work of D'Addona et al. [6], in which the results of heat flow tests conducted for turning Inconel 178 alloy with APC cooling (high-pressure coolant) are presented. Analyzing several studies, it can be stated that FEM is a computational method of great versatility and universality, which is why it is widely used in both science and industry. The boundary element method shares similar characteristics. A good example of turning process simulation using the BEM method is the work of Zhang et al. [7]. The presented research focused on determining the influence of protective coatings of the cutting tool on the distribution of the temperature field in the cutting zone. It should be noted that in both methods, the Johnson-Cook material constitutive model was used. The J-C material model is represented by six numerical parameter values [8]. The J-C material model equation is presented below:

$$\sigma_p = \left(A + B\varepsilon_p{}^n\right)\left[1 + C\ln\left(\frac{\dot{\varepsilon}_p}{\dot{\varepsilon}_0}\right)\right]\left[1 - \left(\frac{T-T_0}{T_t-T_0}\right)^m\right] \tag{1}$$

where A is initial yield stress of materials at reference strain rate and reference temperature; B is strain hardening modulus; C is strain rate hardening parameter; m is temperature softening coefficient, n is hardening index; T_o is room temperature; T_t is melting temperature; T is working temperature; ε_p is plastic strain; and $\dot{\varepsilon}_0$ is reference strain rate.

The literature contains many examples of computer simulations of the cutting process based on the Johnson-Cook material model. Moreover, for the same material, several different sets of numerical data for the J-C material model parameters can be found. Examples of several such parameter sets are shown in Table 1.

Table 1 *Constants for the Johnson-Cook material equation for 316L steel [9]*

Material model	A (MPa)	B (MPa)	n	C	m	$\dot{\varepsilon}_p{}^0$ (s^{-1})	Source
Model 1	514	514	0.508	0.042	0.533	0.001	[10]
Model 2	400	750	0.500	0.040	0.500	1	[11]
Model 3	305	1161	0.610	0.010	0.517	1	[12, 13, 14]
Model 4	305	441	0.100	0.057	1.041	1	[12, 13]
Model 5	312	1114	0.600	0.040	0.632	1	[12]
Model 6	301	1472	0.807	0.090	0.623	0.001	[13, 15]
Model 7	280	1750	0.800	0.100	0.850	200	[13]

All the analyzed articles indicate that the selected J-C material model for simulation is accurate, because it closely approximates the evaluated value to the same value obtained in experiments. Sometimes, the compared quantity is chip morphology; other times, it's cutting forces or contact temperature. Typically, the criterion for evaluating the accuracy of the selected model is the phenomenon (quantity or parameter) crucial for the analyses conducted. This method of selecting material model parameters is very subjective. Therefore, the question arises: how can such parameter selection be conducted consciously and purposefully? To base such a choice on

solid knowledge, one must understand the significance of the values of individual variables in the J-C model and their impact on simulation results.

For this reason, in this article was decided to examine the significance of the values of individual parameters of the J-C material model for the simulation results. Additionally, during the research, an attempt was made to estimate the changes in the values of these parameters based on the results of numerical calculations. In the future, this knowledge will enable better selection and optimization of J-C material model parameters in machining simulations.

2. METHODOLOGY

2.1 EXPERIMENTAL SETUP

Experimental cutting tests were conducted on a setup based on a TUM-35D1 center lathe with a modified drive system (Figure 1). This modification allowed for flexible regulation and adjustment of the spindle speed. The feed was set incrementally.
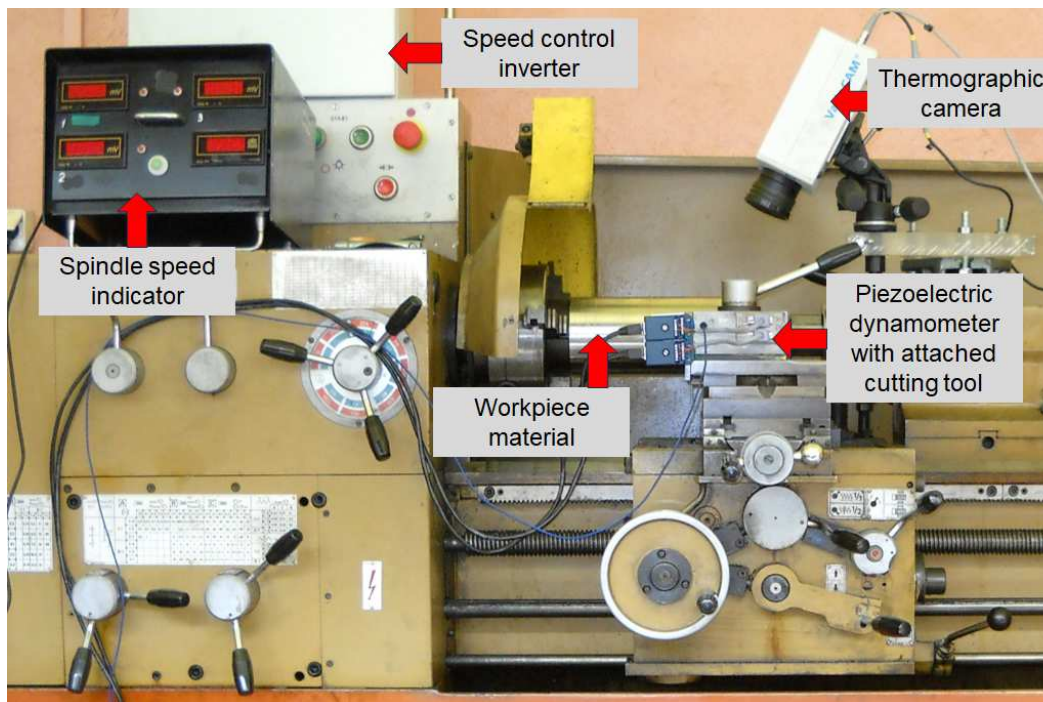

Fig. 1 *General view of the experimental setup [9]*

The components of the total cutting force, contact temperature, and thermographic images of the cutting zone were measured during the tests. A KISTLER 9257B piezoelectric dynamometer with a KISTLER 5019B charge amplifier and NATIONAL INSTRUMENTS NI6062E measurement card was used for force measurement. The average contact temperature was measured using the single-edge natural thermocouple method. Thermographic images were collected using a JENOPTIK VARIOCAM camera with IRBIS3 software.

2.2 WORKPIECE MATERIAL

The workpiece material was austenitic stainless steel AISI 321. This material is frequently used in the energy, chemical, pharmaceutical, and food industries due to its high corrosion resistance and good weldability. Its chemical composition was determined in studies and is shown in Table 2 [9]. The mechanical properties of the AISI 321 are reported in Table 3 [16].

Table 2 *Alloy composition of AISI 321 steel [9]*

alloying element	Mn	Si	P	S	Cr	Ni	Mo
average value	1.63	0.66	0.007	0.014	17.31	9.29	0.36
alloying element	Cu	V	Al	Ti	W	Co	Pb
average value	0.43	0.062	0.025	0.309	0.029	0.116	<0.001
alloying element	Sn	As	B	N	Ca	Fe	
average value	0.010	0.003	0.0013	<0.001	0.0017	69.70	

Table 3 *Mechanical properties of the AISI 321 [16]*

Property	Value
tensile strength (N/mm²)	567
yield strength $R_{0.2}$ (N/mm²)	1080 - 1370
elongation (%)	57
hardness (HB)	164
Poisson's ratio	0.3

2.3 CUTTING TOOL AND MACHINING CONDITIONS

All experimental studies were conducted using a PTNGR 2020-16 tool holder to ensure orthogonal tool positioning. Interchangeable cutting inserts with a flat rake face, TNMA160408, were used as the cutting edge. The specification of the tool's cutting-edge angles is shown in Table 4. The study examined the case of orthogonal, dry cutting of AISI 321 steel with uncoated H10F carbide inserts.

Table 4 *Specification of tool edge angles according to [9]*

Angle	Designation	Value
rake angle	γ_n	-5°
clearance angle	α_n	5°
major approach angle	κ_r	90°
minor approach angle	κ_r'	-
cutting edge inclination angle	s	-6°

Experimental studies of the cutting process were performed on samples in the shape of a cylinder with an undercut that formed a short tube with a wall thickness of 2 mm. The sample was clamped in the chuck with special textolite inserts to isolate the sample electrically from the machine mechanisms. Table 5 shows the technological parameters adopted for experimental tests and FEM simulations.

Table 5 *Technological parameters used in experimental and simulation research*

Machining conditions	Value
cutting speed (m/min)	66.67, 100.00, 133.33
feed (mm/rev)	0.20
cutting width (mm)	2

2.4 COMPUTER SIMULATIONS

DEFORM 2D/3D software was used for simulation studies of the cutting process. The parameters of the J-C equation obtained in the studies were used to best replicate the behaviour of the workpiece material in the chip formation zone in numerical calculations (Table 6). These parameters were determined using the Taylor impact test [9].

Table 6 *Constants for the Johnson-Cook material equation for AISI321 steel [9]*

A (MPa)	B (MPa)	n	C	m	$\dot{\varepsilon}_p^0$ (s^{-1})
258.7	495.3	0.324	0.029	1.097	1.887x10^{-3}

The mechanical, tribological, and thermophysical data of the workpiece material were obtained from tables available in the DEFORM software. All data considered temperature effects. The Cockroft-Latham damage model available in the system was used to describe the decohesion of the workpiece material. The critical value of the Cockroft-Latham model was set to 135, and damage softening to 37%. A shear model was used as the friction model between the tool and the workpiece, which was 0.8. Calculations were performed on a dual-processor HPC server platform with three GPU accelerators (2x Intel Xeon E5-2683 v3, each with 14 cores, 128 GB RAM, 1x Samsung EVO 1TB SSD).

Simulation studies were run for several key parameters of the J-C material model, which greatly affected the final simulation result. Calculations were performed for the following quantities, varied stepwise by ±10%:

- A, yield strength for reference parameters: temperature T_R and strain rate $\dot{\varepsilon}_0$,
- B, n, strain hardening coefficients,
- C, dynamic hardening coefficient,
- T_m, melting temperature.

3. RESULTS AND ANALYSIS

Simulation studies of the cutting process analyzed J-C material models available in the literature for AISI 316L steel, considering it the closest equivalent to the studied AISI 321 steel. Example sets of J-C equation parameters are shown in Table 1. These models, and specifically their stress-strain variations, were compared with each other and against experimental data obtained for AISI 321 steel. Comparing the graphical curves obtained for a temperature of 300°C (Figure 2) and a temperature of 900°C (Figure 3), it is easy to notice that the shapes and slopes of the presented waveforms do not change. Only the vertical position of the observed curves changes. Regardless of the temperature, the curve determined for model 4 (Table 1) is always at the top.

For example, at 300°C, its starting point is around a stress of 400 MPa (Figure 2), while at 900°C, its starting point is much lower, around 200 MPa (Figure 3). Similar changes occur for all other curves. The lowest waveform is obtained for the model 3 curve (Table 1). The starting position of this curve changes from 180 MPa to 70 MPa. The waveform for the experimentally determined model (Table 6) is located centrally among the analyzed curves, regardless of temperature (Figures 2 and 3).
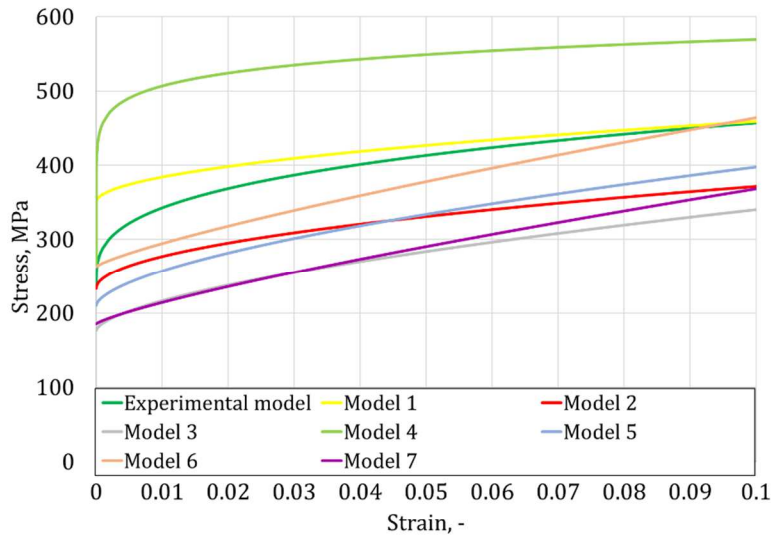

Fig. 2 *View of stress-strain curves at 300°C*
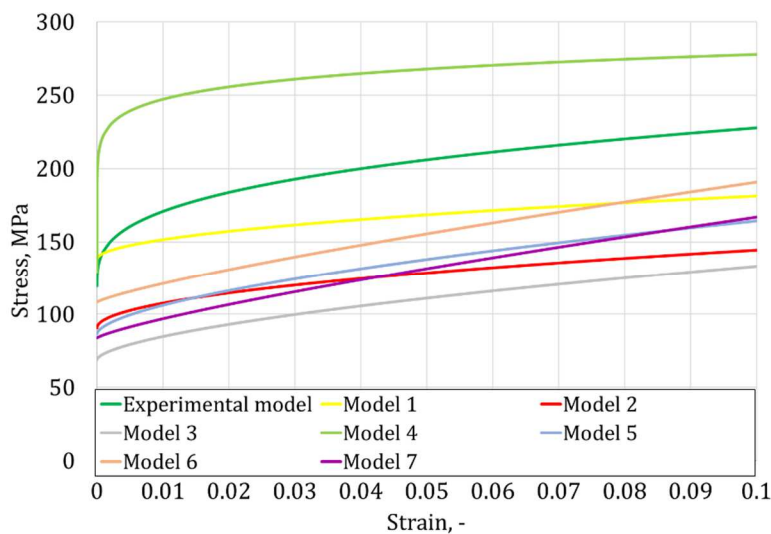
Fig. 3 *View of stress-strain curves at 900°C*

A three-dimensional view of changes in the stress-strain-temperature system (Figure 4) shows that the generated surfaces for different sets of material constants interpenetrate and have different curvatures. It should be noted that all these surfaces were generated from the same material, AISI 316L steel. This raises the question: which of these data sets (Tables 1 and 6) will best reflect the conditions of actual experimental studies, and which set should be chosen for the simulation calculations of the cutting process?

Comparing the results of experimental studies, simulation results for the experimentally measured J-C equation parameters, and simulation results for two selected sets of J-C equation

parameters from the literature indicates that the choice of constitutive equation parameters is crucial for simulation results. For comparisons, the parameter set for model 3 (the highest plane), the experimentally determined data (the middle plane), and the parameter set for model 4 (the lowest plane) were selected. The presented graphs of the main cutting force (Figure 5) and the feed force (Figure 6) indicate that the best agreement with experimental data is shown by simulations performed for the experimentally determined J-C equation parameters (Table 6). In this case, the discrepancy of results ranges from 3 to approximately 15%. For the other two data sets (models 3 and 4), the forces determined in the simulations show significant discrepancies. Results for model 3 are too high, with a difference reaching up to +58%. In the case of model 4, the nature of the cutting force variation is somewhat different from the other cases, showing a constant value throughout the examined range (Figure 5). The difference from experimental studies of the cutting process ranges from -42% to -27%. The feed force waveform shown in Figure 6 exhibits similar changes. The greatest consistency with experimental studies is shown by the calculation results for the J-C model determined in the studies. Differences between these results range from -11% to +1%. In other cases, the differences are, respectively, from +12% to +39% for model 3 and from -30% to -44% for model 4.
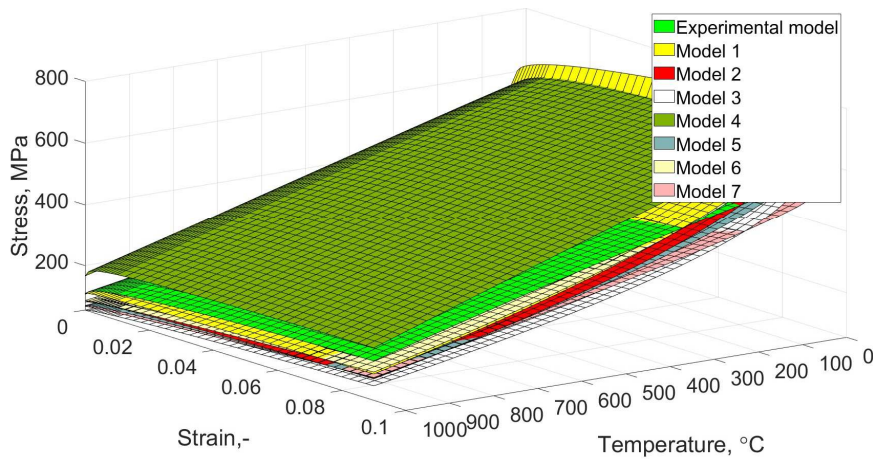

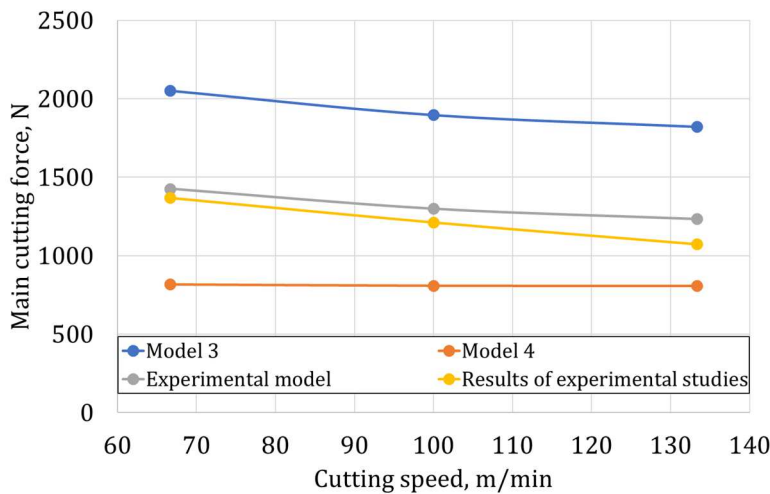**Fig. 4** *View of stress-strain-temperature changes for compared materials*

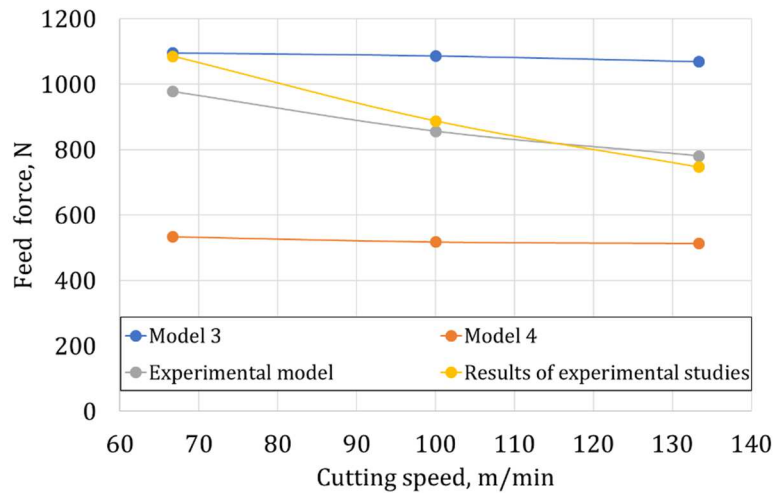**Fig. 5** *Variation of the main cutting force with cutting speed*

Fig. 6 *Variation of the feed force with cutting speed*

A similar nature of changes can be observed in the cutting temperature waveforms shown in Figure 7. The results presented here are the average temperature values determined from the time of stabilization until the end of the cutting process in the FEM simulation. In all cases, the character of the analyzed waveforms is similar. Moreover, as before, a significant similarity was noted between the experimental study waveform and the simulation results using the parameters from Table 6. Discrepancies between these results range from -6% to -8%. For model 3, the deviation in results ranges from +15% to +23%. For model 4, these discrepancies range from -23% to -30%.
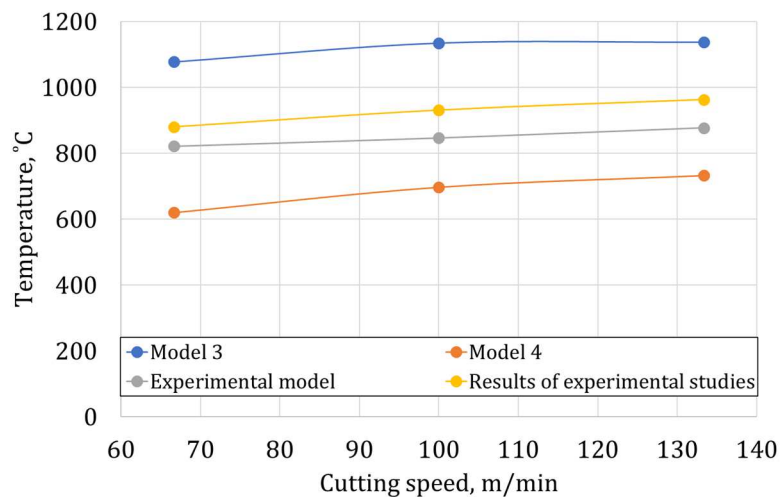

Fig. 7 *Variation of contact temperature with cutting speed*

A different nature of the influence of model parameters on the simulation results is characterized by the distribution of stresses generated in the cutting zone, visible in Figure 8. The comparison indicates that the results obtained for model 3 are significantly too high, with deviations from the measured data ranging from +43% to +53%.
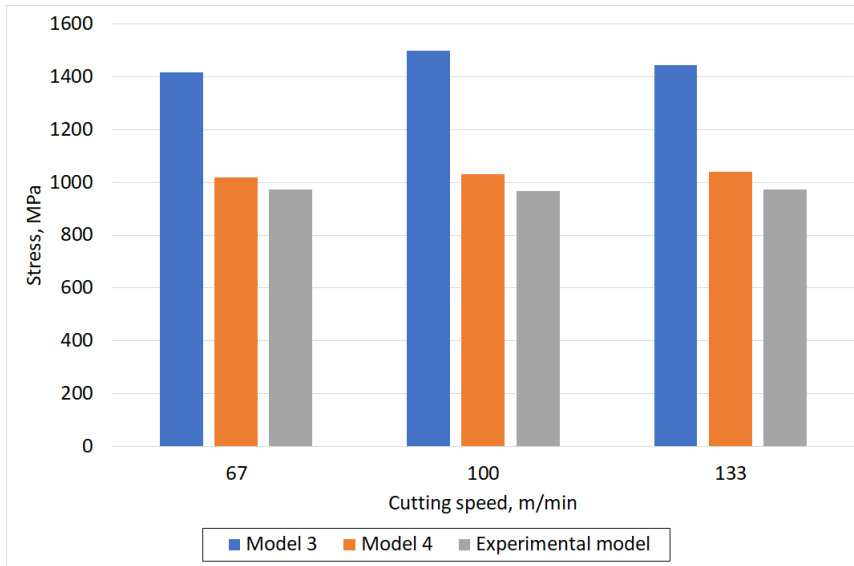
Fig. 8 *Comparison of maximum stress values in the chip formation zone*

The influence of material model parameters on simulation results is a complex issue. The graph shown in Figure 8 does not fully reflect the phenomenon of stress distribution generation in the cutting zone. An example supporting this is the stress fields shown in Figure 9. Comparing these stress fields for three different sets of input data (model 3, model 4, and the experimental model) shows clear significant differences in stress distribution, chip structure, and the chip formation zone. The comparison of the models (Figure 9) indicates that the highest stresses are generated in model 3 and are located on the machined surface. It should be noted that the chip root is wide, and the material is compressed above the cutting zone. The chip itself has not yet formed into its final shape. For model 4, the primary plastic deformation zone is visible. This is where the highest stress area is located. The chip is fully formed, and its flow direction is visible. The chip thickness is significantly smaller than in other cutting zone images analyzed (Figure 9).
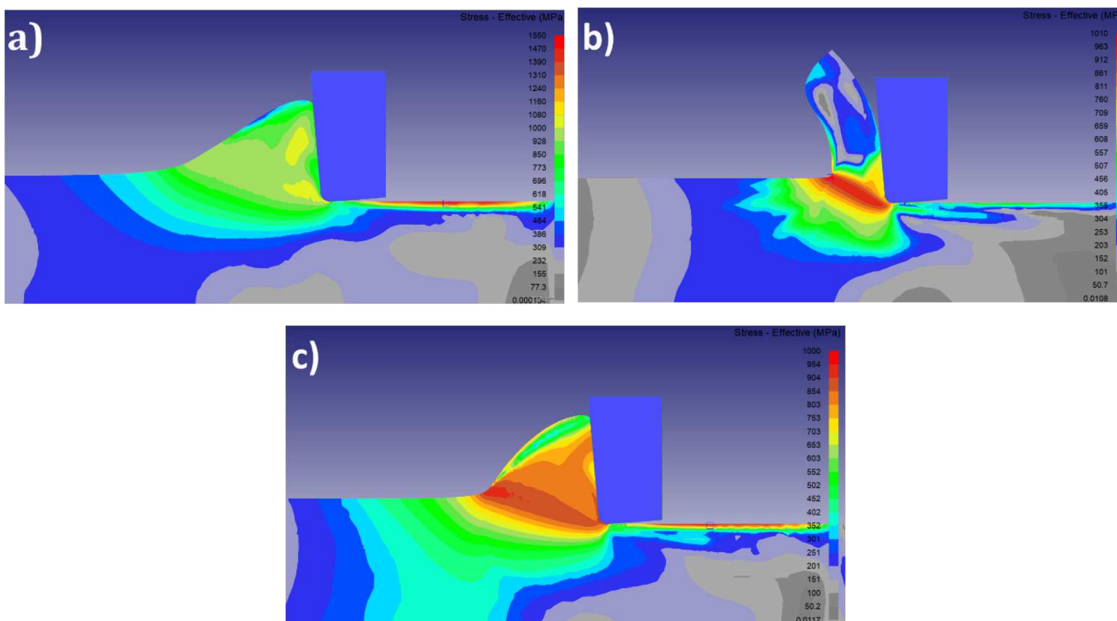

Fig. 9 *Comparison of stress distribution in the cutting zone for a cutting time of 0.00178 s for a) model 3, b) model 4, c) experimental model*

This significant difference in the chip root structure should be understood as a result of different values of parameters *B* and *n*, as these two parameters are responsible for the strain hardening of the workpiece material. Moreover, the final result is also influenced by other equation parameters. For instance, parameter *C* determines the dynamic hardening of the material, while the generated temperature affects the thermal softening of the material. For comparison, using the J-C equation parameters obtained from the conducted experimental studies (Table 6) in the calculations results in a simulation image that is an intermediate version between model 3 and model 4 in shape and dimensions. The area of maximum stress occurrence is more extensive and covers both the chip formation zone and the machined surface.

A series of simulation calculations were run, adopting the parameter values listed in Table 7, to check the actual influence of individual parameters of the Johnson-Cook material equation. These calculations examined how changes in individual parameter values by +10% and -10% affect the shape and positioning of the stress-strain characteristic.

Table 7 *Johnson-Cook material equation parameter values adopted for calculations*

Material model	A (MPa)	B (MPa)	C	n	m	$\dot{\varepsilon}_p^0$ (s^{-1})
Experimental model	258.7	495.3	0.029	0.324	1.097	0.001887
A +10%	**284.6**	495.3	0.029	0.324	1.097	0.001887
A - 10%	**232.9**	495.3	0.029	0.324	1.097	0.001887
C +10%	258.7	495.3	**0.0319**	0.324	1.097	0.001887
C -10%	258.7	495.3	**0.0261**	0.324	1.097	0.001887

The presented calculations indicate that the greatest influence on the positioning of the stress-strain curve is exerted by the yield strength of the workpiece material (Figure 10) and the smallest by the dynamic hardening coefficient (Figure 11). For a temperature of 300°C, a change in parameter *A* (yield strength) by +10% resulted in a deviation of the maximum stresses of about +22%, whereas for a temperature of 900°C, this change was about half as much, only about +10% (Figure 10). A change in parameter A by -10% caused a change in stresses of about -6% for a temperature of 300°C and about -5% for a temperature of 900°C. In contrast, parameter C, which indicates the dynamic hardening coefficient, causes very slight changes in the observed stress-strain characteristics. Regardless of the process temperature, a change in parameter *C* by +/-10% results in a change in maximum stresses of only about +/-1% (Figure 11).

To summarize, each parameter exhibits a different intensity of influence on the stress-strain characteristic. However, neither the shape of the analyzed curves nor their slope changes. Only the vertical location of the curves changes. However, the conducted studies do not provide a complete picture of the analyzed phenomena. Therefore, simulation studies of the cutting process have already been undertaken, in which the influence of individual parameters of the Johnson-Cook constitutive equation on the distribution of temperature, stress, strain, and chip morphology is being determined.
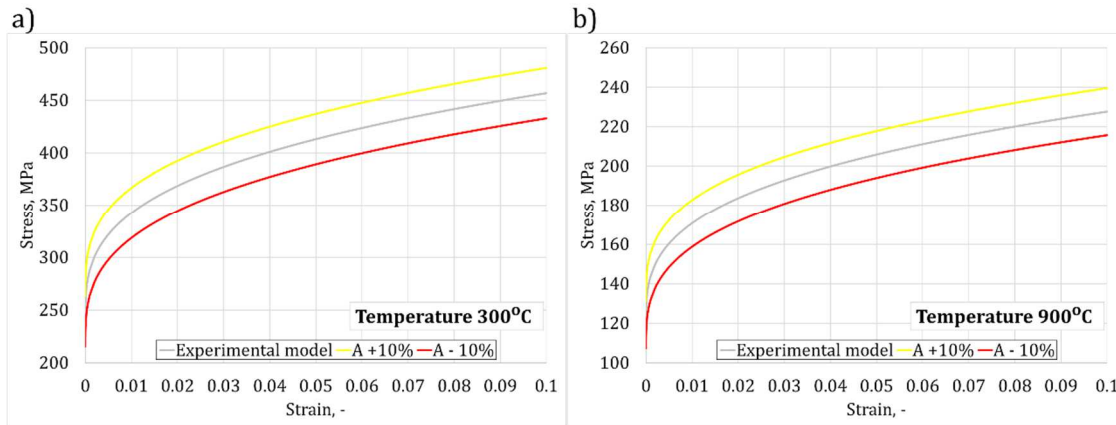
Fig. 10 *The impact of changes in the yield strength of the workpiece material (parameter A) on the stress-strain curves for temperatures of a) 300˚C and b) 900˚C*
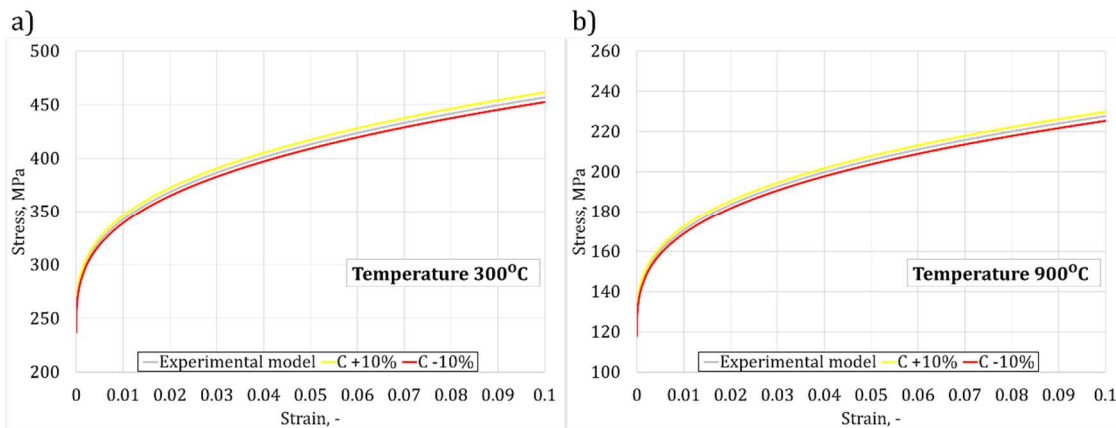

Fig. 11 *The impact of changes in the dynamic hardening coefficient (parameter C) on the stress-strain curves for temperatures of a) 300˚C and b) 900˚C*

4. CONCLUSION

The conducted studies and analyses lead to the formulation of the following conclusions:

- Based on experimental studies and calculations, it is possible to establish more than one set of data that satisfies the Johnson-Cook equation, but each of these data sets yields different results in numerical calculations.

- The Johnson-Cook material model shows the largest sensitivity to changes in yield strength (parameter A), as a change in this parameter in the range of +/-10% results in a change in maximum stresses of about +22% and -6%.

- The same material model shows the least sensitivity to changes in parameter C (dynamic hardening coefficient), as a change in this parameter in the range of +/-10% results in a change in maximum stresses of about +/-1%.

- As the process temperature increases from 300℃ to 900℃, the influence of individual parameters on the stress-strain characteristic decreases by about half.

- There is a need to conduct further, more extensive studies to fully understand the influence of the J-C material model parameters on the results of computer simulations of the cutting process.

5. REFERENCES

[1] Grzesik, W., *Advanced Machining Processes of Metallic Materials: Theory, Modelling and Applications*, Copyright © 2017 Elsevier, ISBN 978-0-444-63711-6.

[2] Łatuszyńska, M., Metody symulacji komputerowej – próba klasyfikacji logicznej, *Studies & Proceedings of Polish Association for Knowledge Management*, Nr 41, pp. 163-176, 2011.

[3] W. Grzesik, W., Bartoszuk, M., Prediction of Temperature Distribution in the Cutting Zone Using Finite Difference Approach, *International Journal of Machining and Machinability of Materials*, Vol. 6, No. 1-2, pp. 43-53, 2009. https://doi.org/10.1504/IJMMM.2009.026926

[4] Grzesik, W., *Podstawy skrawania materiałów konstrukcyjnych*, Wydawnictwo WNT 2018, ISBN 978-83-01-19919-7.

[5] Wu, L., Liu, J., Ren, Y. et al., 3D FEM simulation of chip breakage in turning AISI1045 with complicate-grooved insert, *International Journal of Advanced Manufacturing Technology*, Vol. 108, pp. 1331–1341, 2020. https://doi.org/10.1007/s00170-020-05460-1

[6] D'Addona, M.D., Raykar, S.J., Thermal Modeling of Tool Temperature Distribution during High Pressure Coolant Assisted Turning of Inconel 718, *Materials*, Vol. 12(3), p. 408, 2019. https://doi.org/10.3390/ma12030408

[7] Zhang, Y., Gu, Y., Tzong, J., Chen, J.T., Boundary element analysis of the thermal behaviour in thin-coated cutting tools, *Engineering Analysis with Boundary Elements*, Vol. 34(9), pp. 775-784, 2010. https://doi.org/10.1016/j.enganabound.2010.03.014

[8] Johnson, G.R., Cook, W.H., A constitutive model and data for metals subjected to large strains, high strain rates and high temperatures, Proceedings 7th International Symposium on Ballistics, The Hague, 541-547, 19-21 April 1983.

[9] Bartoszuk, M., Modelowanie przepływu ciepła i rozkładu temperatury w strefie skrawania dla ostrzy węglikowych, *Oficyna Wydawnicza Politechniki Opolskiej*, Opole 2013, ISBN 978-83-64056-05-5.

[10] Tounsi, N., Vincenti, J., Otho, A., Elbestawi, M.A., From the basic mechanics of orthogonal metal cutting toward the identification of the constitutive equation, *International Journal of Machine Tools and Manufacture*, Vol. 42(12), pp. 1373-1383, 2002.

https://doi.org/10.1016/S0890-6955(02)00046-9

[11] Miguélez, M.H., Zaera, R., Molinari, A., Cheriguene, R., Rusinek, A., Residual Stresses in Orthogonal Cutting of Metals: The Effect of Thermomechanical Coupling Parameters and of Friction, *Journal of Thermal Stresses*, Vol. 32(3), pp. 269-289, 2009.

https://doi.org/10.1080/01495730802637134

[12] Chandrasekaran, H., M'Saoubi, R., Chazal, H., Modelling of Material Flow Stress in Chip Formation Process From Orthogonal Milling and Split Hopkinson Bar Tests, *Machining Science and Technology*, Vol. 9(1), pp. 131-145, 2005.

https://doi.org/10.1081/MST-200051380

[13] Umbrello, D., M'Saoubi, R., Outeiro, J.C., The influence of Johnson–Cook material constants on finite element simulation of machining of AISI 316L steel, *International Journal of Machine Tools and Manufacture*, Vol. 47(3–4), pp. 462-470, 2007.

https://doi.org/10.1016/j.ijmachtools.2006.06.006

[14] Malakizadi, A., Oberbeck, J.N., Magnevall, M., Krajnik, P., A new constitutive model for cutting simulation of 316L austenitic stainless steel, *Procedia CIRP*, Vol. 82, pp. 53-58, 2019. https://doi.org/10.1016/j.procir.2019.04.064

[15] Uçak, N., Aslantas, K., Çiçek, A., The effects of Al2O3 coating on serrated chip geometry and adiabatic shear banding in orthogonal cutting of AISI 316L stainless steel, *Journal of Materials Research and Technology*, Vol. 9(5), pp. 10758-10767, 2020.

https://doi.org/10.1016/j.jmrt.2020.07.087

[16] Fezai, N., Chaabani, L., Niang, N.F., Bin Haamsir, M.H., Fontaine, M., Gilbin, A., Picart, P., Characterization of friction for the simulation of multi-pass orthogonal micro-cutting of 316L stainless steel, *Procedia CIRP*, Vol. 108, pp. 845-850, 2022.

https://doi.org/10.1016/j.procir.2022.03.130